Bending Stress Analysis of Worm Wheel of Winch Machine Gearbox Using Experimental and FE Analysis

[1]Mr. Rahul R. Londhe , [2]Prof. J. S. Shitole, [3]Prof.B.R.Valkunde

[1]PG Student, [2, 3]Assistant Professor

Dattakala Group of Institutions Faculty of Engineering, Maharashtra, India

ABSTRACT

Gears are most frequently used components to be found in rotating machinery used in various industrial applications. Even though its failure can disturb the complete production in a plant resulting in unscheduled downtime and production losses. Also, the detection of gear failure and its cause at correct time is important otherwise its sustain bigger loss.

So this Project deals with study of gears failures analysis by using various methods used in industries and the techniques used to improve gear quality before manufacturing.

In this project study we provide reasons, solutions and prevention methods and ways to avoid gear failure.

Keywords:- *Worm Gear, Stress analysis ,FEA , 3D Photoelasticity, Lewis equation,*

1.INTRODUCTION

Worm Gearing

Worm gears are that types of gears which are used to transmit power between two non-intersecting, non-parallel shafts. These gears are generally at right angles to each other. It consists of worm and worm wheel. The worm is threaded screw and worm wheel is toothed gear. The figure shows meshing of worm and wheel. The teeth on the worm wheel envelope the treads on worm. This gives line contact between mating parts. In other types of gears, the drive can be given to any one of the two mating parts. But in worm gears, the drive can be given to only worm. The worm can rotate worm wheel but worm wheel cannot rotate worm.

Fig.1 Worm Gear

Failure of Gears

Failure of gears may be classified into four categories:

- Surface fatigue (pitting)
- Wear
- Plastic flow
- Breakage

The appearance of the various distress and failure modes can differ between gears that have through hardened teeth and those that have surface hardened teeth. These differences result from the different physical characteristics and properties and from the residual stress characteristics associated with the surface hardened gearing.

2.Problem Statement

The worm and worm wheel is used in winch machine gearbox. During operation it was observed that the worm wheel fails due to load coming on the teeth. The failure starts at the central thickness of tooth and continues up to the root of the tooth. At the initial stage of failure, the tooth was going in plastic deformation and then crack was occurring at the central thickness. The failure was occurring once within operational period of about 15 days. So the industry had to replace the worm wheel which was not cost effective. The material of worm is hardened steel and the material of the wheel is phosphor bronze PB2 having approximate composition in percentages as (Cu = 85, Sn = 12, Zn = 0.3, Pb = 0.5, P = 0.4 and other = 2).

The calculation of stresses of worm wheel at tooth thickness is a three dimensional problem. Thus we can analyze the stress pattern by using 3D Photoelasticity techniques and finite Element analysis technique.

3.OBJECTIVES AND WORKING METHODOLOGIES

Objectives:-

Following are the main objectives of dissertation work.

1. To evaluate bending stress distribution at tooth root of wheel using experimental analysis using 3D photo elasticity.
2. To evaluate bending stress distribution at tooth root of wheel using FE Analysis using ANSYS.
3. To validate experimentally obtained results with FEA results and plotting final results.
4. To give design solutions to the Advance Engineer to improve life of worm wheel.

4.LITERATURE SURVEY

In spite of the wide use of worm gear drives, only few papers have been published on analysis and load distribution calculation of worm gears. Previous works addressing worm gear analysis published by some authors is as follows.

1. Prashant Patil, Narayan Dharashiwkar, Krishnakumar Joshi and Mahesh Jadhav have discussed about 3D Photoelastic and Finite Element Analysis of helical gear. They have discussed an industrial problem which uses spreading machine to spread bagasse. This spreading machine has Positive Infinite Variable (PIV) gearbox which contains helical gears. In working condition, helical pinion fails due to load coming on the teeth. It seemed that the failure was due to stress concentration and bending stresses at tooth root of gear. The calculation of maximum tensile stress at tooth root was a three dimensional problem. Thus they have analyzed the stress pattern by using 3D Photo elasticity techniques. Also they have verified obtained results with FEA. They have found out that the failure of helical gear of PIV gear box may be due to improper alignment or due to improper heat treatment process during teeth hardening.

2. Bhosale Kailash C. and Dongare A. D. have discussed about an experimental and finite element method of analysis. In their paper, they have analyzed bending strength of helical gear using photoelasticity technique. The experimentally obtained results are verified with finite element results. The conclusion of their work have proved that the error in maximum bending stress calculated by both, experimental and finite element technique, is only about 2.02%. Thus it clears that these both methods are best suitable for bending stress analysis of gears.

3. W. T. Moody and H. B. Phillips have published various techniques of analysis of mechanical component in Photoelastic and Experimental Analog Procedures Engineering Monograph No. 23. Along

with the theory of technique, they have explained all details including material requirement, instrument used for analysis, calibration techniques, the polariscope, nature of light and plane polarization, 3D photoelasticity, the photoelastic interferometer, the babinet compensator, the beggs deformeter, the electrical analogy tray, the membrane analogy, photoelastic materials and model preparation, photoelastic model loading frame assembly.

4. Rexnord Industries, LLC, Gear Group , has given all the details regarding gear distress and failure modes, surface fatigue i.e. pitting and spalling, wear, degrees of wear, types of wear, miscellaneous wear modes, plastic flow, breakage, failure associated with processing along with reasons for failures and preventive action to be taken so as to avoid the failures in their publication named Failure Analysis Gears-Shafts-Bearings-Seals.

5. Dr. V. B. Sondur and Mr. N. S. Dharashivkar have discussed about theoretical and finite element analysis of load carrying capacity of asymmetric involute spur gears. In this paper, they have presented a method for investigating the bending stress at the critical section of "Asymmetric Involute spur Gear". The gears with different pressure angle have been modeled by using CATIA software and analysis was carried out. The results obtained by theoretical method have been verified by using ANSYS. From their work they have proved that bending stress can be minimized up to 20% by increasing pressure angle from 20° to 35°. Thus from their work it is clear that FEA can be the best technique for designing and analyzing mechanical component.

6. Pravin M. Kinge, Prof. B.R. Kharde and Prof. B.R. Borkar have analysed gearbox used in sugar industry. The main objective of analysis was to improve the life of the gear. The reason found for failure of the gear was due to wear of gear teeth edges. This is caused due to high stress concentration along gear teeth edges. To relieve these stress concentration three modifications in the design were done using ANSYS and again stress analysis of the modified gears carried out. The three design modifications were done as first, the edges of the gear teeth were tapered by an angle of 20^0, second, making groove in the gear wheel and third, making holes at the roots of the gear teeth. They have proved that the expected increase in life of the gears of the gearbox would be three years.

7. Gavril Ion has discussed tooth's tensions analysis of face worm gears with cylindrical pinion development of FEA. He has proposed tooth's tension in lapping process for worm face gear. In this paper, the stress analysis of the gear drive is performed using a three-dimensional finite element analysis. The developed simulation is illustrated with numerical examples. This complex and intuitive simulation was created with CAD-CAM, MATH-CAD and FEM support.

8. William L. Janninck has discussed about the contact surface topology of worm gear teeth. In a mating worm and warm. gear set, the inspection of the worm member is accomplished by available analytical inspection procedures. The mating enveloping worm gear with its distorted tooth surfaces is generally accepted by the contact pattern developed while running the gear with a qualified worm. These patterns will only show that area with a minimal separation between the worm and worm gear tooth surfaces and the actual separation beyond the contact area are unknown. A mathematical modeling procedure has been developed to predict the initial contact pattern. As well as the surface separation topology over the entire worm gear tooth surface equations and procedures are presented to permit an analysis for any gear set. He has also explained about production ways of gears. There are five popular ways to make a worm-Thread chasing, Thread milling, Thread grinding, Hobbing and Roll forming. The Worm gear Member can be made by gear hobbing processes i.e. Radial feed and Tangential feed.

5.THEORETICAL ANALYSIS

Terminologies of Worm Gears

pair of worm gears is specified and designated by four main quantities as follows.

$z_1 / z_2 / q / m$

The existing gear has designation as follows, 1/60/12.18/2.8

Existing Gear Parameters

The following table shows the gear parameters which are provided by company. The below mentioned values are confirmed from reference books and they found correct

Sr.	Parameters	Notations	Values
1	Number of starts on	z_1	1
2	Number of teeth on	z_2	60
3	Diametral quotient	q	12.18 mm
4	Module	m	2.82 mm
5	Centre distance	a	101.60
6	Lead angle	γ	4.69°
7	Pressure angle	α	20°
8	Pitch Circle Diameter	d_1	34.36 mm
9	Addendum of worm	h_{a1}	2.82 mm
10	Dedendum of worm	h_{f1}	3.38 mm
11	Outside diameter of	da_1	40 mm
12	Root diameter of worm	df_1	28.72 mm
13	Axial pitch	p_a	8.859 mm
14	Length of worm	b_1	60.74 mm
15	Tooth thickness of	s	4.43 mm
16	Top Clearance	c	0.564 mm
17	Pitch Circle Diameter	d_2	168.84
18	Throat diameter of	da_2	174.84
19	Addendum of worm	h_{a2}	2.82 mm
20	Dedendum of worm	h_{f2}	3.38 mm
21	Outside diameter of	d_A	177.30
22	Root diameter of worm	d_{f2}	163.56 mm
23	Face width	b_2	25.08 mm

Force Analysis of Worm Gears

The three main components of resultant tooth force acting on worm and worm wheel are as follows,

$(P)_t$ = Tangential component (N)
$(P)_a$ = Axial component (N)
$(P)_r$ = Radial component (N)

- Torque transmitted is given as below.

$$\text{Mt} = \frac{60 * 10^6 * 5}{2 * 3.14 * 1440} = 33157.27 \text{ Nmm}$$

- Rubbing Speed,

$$v_s = \frac{\pi d_1 n_1}{60000 \cos\gamma}$$

$$v_s = \frac{\pi * 34.36 * 1440}{60000 \cos 4.69}$$

$$v_s = 2.599 \text{ m/s}$$

- Coefficient of friction, $\mu = 0.031$---(coefficient of friction Vs Rubbing speed graph)

Forces calculations for worm,

- Tangential component

$$(\text{P1})\text{t} = \frac{2\text{Mt}}{\text{d1}}$$

$$= \frac{2 * 33157.27}{34.36}$$

$$= 1929.99 \text{ N}$$

- Axial component

$$(\text{P1})\text{a} = (\text{P1})\text{t} * \frac{(\cos\alpha \cos\gamma - \mu \sin\gamma)}{(\cos\alpha \sin\gamma + \mu \cos\gamma)}$$

$$= 1929.99 * \frac{(\cos 20 \cos 4.69 - 0.031 \sin 4.69)}{(\cos 20 \sin 4.69 + 0.031 \cos 4.69)}$$

$$= 16732.57 \text{ N}$$

- Radial component

$$(\text{P1})\text{ r} = (\text{P1})\text{t} * \frac{\sin\alpha}{(\cos\alpha \sin\gamma + \mu \cos\gamma)}$$

$$= 1929.99 * \frac{\sin 20}{(\cos 20 \sin 4.69 + 0.031 \cos 4.69)}$$

$$= 1464.83 \text{ N}$$

Forces calculation for worm wheel,

- Tangential Force, $(P_2)_t$ = 16732.57 N
- Axial Force, $(P_2)_a$ = 1929.99 N
- Radial Force, $(P_2)_r$ = 1464.83 N

Theoretical Analysis by Lewis Equation

- The velocity factor is given by $\sigma_b = P_t / (C_v\, b\, \pi\, m_n\, Y)$

$$Cv = \frac{}{(6 + v)}$$

where *v* is the peripheral velocity of the worm gear in m/s.

$$v = \frac{\pi * \text{d2} * \text{N2}}{60 \times 1000}$$

$$v = \frac{\pi * 168.84 * 24}{60 \times 1000}$$

v= 0.2121 m/s

Therefore, Velocity factor, *Cv* = 0.9658

- Face width is given by equation, $b = 0.73 \times d_1$

$= 0.73 \times 34.36$

b = 25.08 mm

- Normal module, m_n

$m_n = m_a / \cos\alpha$

where m_a is axial module, $m_a = d_1 / 3\pi$

$= 34.36/3\pi$

$m_a = 3.645$

Therefore, normal module is $m_n = 3.645/ \cos 20$

m_n = 3.878 mm

- The tooth form factor or Lewis factor (*Y*),[11]

When $Z_1 + Z_2 > 40$, then for 20^0 pressure angle, *Y* = 0.392,

Therefore, *Y* = 0.392

Therefore according to Lewis equation,

$\sigma_b = P_t / (C_v\, b\, \pi\, m_n\, Y)$

$\sigma_b = 16732.57 / (0.9658 \times 25.08 \times \pi \times 3.878 \times 0.392)$

$$\sigma_b = 144.64 \text{ N/mm2}$$

The bending stress value is 144.64 N/mm^2. The ultimate tensile strength of the phosphor bronze (PB2) material is 320 N/mm^2. Therefore with reference to these results, it can be stated that, the design of worm wheel is safe as bending stress value is far less than the ultimate tensile strength of the PB2 material. The factor of safety is about 2.21.

Also the hardness of the phosphor bronze PB2 is 110 BH, which is acceptable value, thus it states that the gear material used is suitable for respective application.

6.EXPERIMENTAL ANALYSIS (3D PHOTOELASTICITY)

Principle of Photo elasticity

Photo elasticity is an experimental technique for analysis of stress and strain that is particularly useful for components having complicated geometry, complicated loading conditions, or both. For such cases, analytical methods may be difficult or impossible, and analysis by an experimental approach maybe more correct. Problems involving three-dimensional geometry, multiple-component assemblies, dynamic loading and inelastic material behavior can be experimental analyzed.

Stress Optic Law

In a crystal, velocity of propagation of light at any point depends on direction of propagation and can be represented by ellipsoid. This is equal to saying that the index of refraction at point depends on the direction and can be represented by means of ellipsoid called index ellipsoid. In solids which become doubly refractive under stress, Maxwell found that the principal axes of index ellipsoid coincide with principal stress axes at the point considered. If n_o is the refractive index of unstressed model, and n_1 ,n_2, n_3 principle indices of refraction at a point of the model under stress, then the relation between n_o and $n_1, n_2 n_3$ bear similarities with the generalized Hook's law.

Now if ϵ_1 , ϵ_2, and ϵ_3 are principal strains and σ_1 , σ_2 ,σ_3 are the principal stresses, then

$l_1 - l_0 = l_0\epsilon_1 = (l_0/E) \sigma_1 - \nu l_0 / E (\sigma_{2+} \sigma_3)$

$l_2 - l_0 = l_0\epsilon_2 = (l_0/E) \sigma_2 - \nu l_0 / E (\sigma_{3+} \sigma_1)$

$l_3 - l_0 = l_0\epsilon_3 = (l_0/E) \sigma_3 - \nu l_0 / E (\sigma_{1+} \sigma_2)$

Where l_1, l_2 , l_3 are linear dimensions of cubical element of sides l_0.

Similarly Maxwell's stress-optic law can be stated as;

$n_1 - n_0 = c_1\sigma_1 - c_1 (\sigma_{2+} \sigma_3)$

$n_2 - n_0 = c_1\sigma_2 - c_2 (\sigma_{3+} \sigma_1)$

$n_3 - n_0 = c_1\sigma_3 - c_3 (\sigma_{1+} \sigma_2)$

Where c_1 is called the direct stress-optic coefficient and c_2 called the transverse stress-optic coefficient. Above equations are the fundamental relations linking stresses with observed optical effects and are called the stress-optic laws. If one takes the differences of these equations, the results are

$n_1 - n_0 = (c_1 + c_2) (\sigma_1 - \sigma_2) = 2c\tau_3$

$n_2 - n_0 = (c_1 + c_2) (\sigma_2 - \sigma_3) = 2c\tau_1$

$n_3 - n_0 = (c_1 + c_2) (\sigma_3 - \sigma_1) = 2c\tau_2$

Where, τ_1, τ_2, τ_3 are the principal shears at the point considered

Procedure for 3D Photo elasticity

The general procedure followed for carrying out 3D photo elasticity is listed below. Each of these activities is explained in detail along with actual dissertation work.

a) Preparation of Model

- Preparation of Pattern.
- Preparation of Rubber Mold.
- Casting photo elastic material model.
- Casting of calibration disc.

b) Designing and developing the loading frame to simulate actual loading conditions.

c) Stress freezing.

d) Slicing of model.

e) Stress analysis

Preparation of Model

The accuracy of photo elastic model has got the major effects on the results obtained.

Therefore preparation of the model bears its own importance in the whole problem of photo elastic stress analysis. The preparation of a model is a sort of technique which needs not only great care, but a lot of experience and practice.

A] Preparation of Pattern

We are using photo elasticity technique for analyzing three dimensional stress patterns in actual component. It can be the case that the component may be large in size. Thus we cannot go for analysis of actual larger component. Hence we have to make prototype of required size and then we can analyze that prototype. The obtained results will be calibrated to actual component. In this dissertation, the wheel itself has been used as pattern as the dimensions can be acceptable. The following figure (10) shows the photograph of actual worm wheel.

Fig.2:- Worm Wheel as a Pattern

B] Preparation of Rubber Mold

For casting out photoelastic material model, the mold should be prepared. The mold is generally prepared out of synthetic rubber material. In this dissertation, the mold is prepared out of a synthetic rubber, sylartivi 11.

Fig.3:- Curing of Rubber Mold and Split Mold

Firstly the wooden frame was made of dimension (200×200×65mm). Then bottom side of wooden frame was covered with the glass and sealed it using grease. Then petroleum jelly was applied on the periphery of the worm wheel so as to easy removal of wheel after curing of synthetic rubber. Next the worn wheel was placed at the centre of the wooden frame. The synthetic rubber was mixed with the catalyst. The catalyst should be mixed in proper proportion with synthetic rubber. The proportion of rubber and catalyst was taken as 100: 2.4. Thus 3000 gm of Sylartivi and 72 gm of catalyst was been randomly taken. After mixing catalyst in the rubber, the mixture was stirred in proper and in uniform way for 10 minutes. The stirring has its importance so as to get uniform material of the mold. The next step is to pour the mixture in the wooden frame. The pouring of mixture should be uniform so that there should not be formation of air pockets which can lead to distortion of rubber mold. After pouring the mixture, that model was kept for about 7 days for proper curing.

After 7 days of curing, the pattern was taken out from the rubber mold. Removing pattern from the rubber mold was very difficult task. As the geometry of teeth of wheel is not axial, we cannot remove the pattern directly by pressing. Thus the wooden frame was firstly opened and the solid mold was cut using normal cutter in to three pieces. Thus it became the split mold. Then the pattern was removed. The figure (b) above shows rubber mold kept for curing and split mold.

C] Casting Photo elastic Material Model

There are several photo elastic materials those can be used for this work. The casting of photo elastic model out of rubber mold is very tedious task. The rubber mold was divided into three parts. Therefore for casting photo elastic model out of it, the wooden box was rejoined. Then petroleum jelly was applied on inner surface of total rubber mold for easy removal of model after curing. The joined rubber mold was placed in wooden box and the box was tightened assuring leak proof joints.

Then epoxy resin ARALDITE CY-203-1 IN was taken for casting photo elastic model. We cannot directly use the epoxy resin alone. The hardener should be mixed so as to solidify the epoxy resin. In this dissertation, HY-951 hardener has been used. The proportion of mixture was 100:7. I had taken 800 gm of Araldite and 56 gm of hardener. The mixture was stirred for 10 minutes very slowly in uniform direction and them that mixture was poured in the rubber mold. The mixture was placed for about 1 month so as to cure properly. After a month, the wooden box was disassembled and photoelastic model was taken out of the rubber mold. The following figure (12) shows the actual photograph of photoelastic model.

Fig.4:- C Photograph of Photo elastic Model

D] Casting of calibration disc

The casting of circular disc was taken so as to find out material fringe value by following the same procedure as explained for wheel.

Designing and Developing the Loading Frame

Designing the loading frame has its own importance. In photo elasticity technique, we must know the actual working condition in which component is working. Unless we know the working condition, we cannot go for accurate analysis.

the photo elastic model is taken out from rubber mold and cured properly, the next step is to go for stress freezing method. The locking of stresses is important when it is the case of three dimensional analyses. Hence loading frame is necessary to load the component to simulate its actual working conditions. Designing and developing the exact loading frame is important because if we fail to do so, we will not be able to find out results at our point of interest. The loading frame must be such that we should able to transmit required torque from one member to another.

The worm wheel taken for analysis is being used in the winch machine gearbox. The figure (a) shows actual photograph of winch machine gearbox. The shafts of worm and worm wheel are fixed with help of bearings in the gearbox.

Fig.5:- Photograph of Winch Machine Gearbox

The frame was made using mild steel angles. The following figure (13) is the actual photograph of loading frame. Both the shafts are fixed into bearings. The bearing housings are bolted to the frame. As we have to analyze the worm wheel, we have to develop fringe pattern in the wheel. Thus the torque required to produce fringe pattern in the wheel must be transferred from worm to worm wheel. Many trials were carried out for designing and developing the frame. Finally one design is finalized which is shown in figure below. Here the worm shaft is provided with lever which is attached for application of load and the rotation of the wheel is restricted by providing a stopper.

Fig.6:- Photograph of Designed Loading Frame

Stress Freezing

After mounting worm gear assembly on loading frame, the loading frame was placed in stress freezing oven for locking stresses up to 36 hrs. The calibration disc was also placed into oven along with the loading frame. Trial and error method has been carried out for deciding load to apply on a model. The experiments has been carried out for 2 kg load , 3 and 4 kg load & it was found that 4 kg load was required to produce adequate no. of fringes.

Slicing

If a three dimensional photo elastic model is observed in a polariscope, the resulting fringe pattern cannot be interpreted. The light passing through the thickness of the model integrates the stress difference σ_1-σ_2 over the length of the path of the light so that little can be concluded regarding the state of stress at any point. To avoid this difficulty, the three dimensional model is usually sliced to remove planes of interest which can then be examined individually. In studies of this type it is assumed that the slice should be sufficiently thin in relation to the size of model to ensure that the stresses do not change in either magnitude or direction through the thickness of the slice. The particular slicing plan employed in sectioning a three dimensional photoelastic model will depend upon the geometry of the model and the information being sought in the analysis.

Fig.7:- Photograph of Slicing the Model

The slices were cut by employing horizontal milling machine with high speed (360 rpm) and slicing saw of 1.5mm thickness. The direction chosen for slicing the model plays an important role. Because of symmetrical shape of the model and symmetrical loading, it was decided to slice longitudinal. Sufficient amount of cutting oil is spread at the time of cutting as coolant. Slice thickness was kept about 3mm.

Stress Analysis

A] Observation under Polariscope

1) To find out isoclinic parameters at various points.

- Confirm the mark line is in line with a mark P on QWP by rotating QWP using knob.
- Confirm that the pointer on analyzer plate scale reads 0.
- See that main pointer reads 0.
- Load the model in the loading frame by applying light load so that only isoclinic fringes will appear. [Use ring model]
- Switch on the white light.
- Observe the model. You will find black colored wide, brush like, fringes over the model. These are isoclinic fringes i.e. principal stress directions indicating fringes. The locus of points joining centre points of fringes is the points on the model, which has isoclinic value of 0. i. e. one of the principal stresses is vertical and other is horizontal.
- Rotate all 4 plates in synchronization by say 150 (or any angle in steps of desired Isoclinic fringe resolution). Now orientation of fringes will change and new pattern will involve. All the centre points of black fringes will be inclined by 150 to vertical and 150 to horizontal, both being in the plane of the model.
- In this way isoclinic parameters for all points on model surface can be determined. In white light, isoclinic fringes are black in color and isochromatic fringes are colored. Therefore both can be separated easily. But the isochromatic fringes having zero order is black. This can be identified separately by rotating all the plates in synchronization due to which only isoclinics will move during this rotation while zero order isochromatic will not move.

2) To analyze model for magnitude of principal stress difference at all points. [Ring model]

- Load the model to full simulated load through 45^0 opposite to each other.
- Rotate QWP so as to get circular Polariscope arrangement.

- Put on white light initially. Now isoclinic fringes are absent. The black fringes indicate the zero order fringes. If maximum order of fringe is more than 4, fringes will not be sharp, as they will diffuse in each other. In that case use monochromatic light, which will show fringes distinctly.
- Note down fringe order at the point of interest.

Following table shows the values for the colors produced in a dark field white light source polariscope.

Table1:- Fringe order

Colors	Fringe Order
Black	0
Grey	0.28
White	0.45
Yellow	0.60
Orange	0.79
Red	0.90
Tint of passage	1.00
Blue	1.06
Blue green	1.20
Green Yellow	1.38
Orange	1.62
Red	1.81
Tint of passage 2	2.00
Green	2.33
Green Yellow	2.50
Pink	2.67
Tint of passage 3	3.00
Green	3.10
Pink	3.60
Tint of passage 4	4.00
Green	4.13

B] Material Fringe Value Using Calibration Disc

The material fringe value is defined as number of fringes produced per unit load. The material fringe value is the property of the model material for a given wavelength (λ) and thickness of the model (h).

Here the circular disk subjected to dimensional compressive load is employed as a calibration model. The circular disc of diameter 50 mm and thickness 6 mm was used to find material fringe value. This circular disc was loaded under compression by special fixture as shown in figure. A compressive load of 2Kg was applied to find material fringe value. This circular disc was also subjected to same stress freezing cycle as that for the model. Viewing through dark field of circulated polariscope, locked isochromatic fringe pattern was observed.

By using following equation, material fringe value (F_σ) at critical temperature was found out.

$$F_\sigma = \frac{8 \times P}{\pi \times D \times N}$$

P=Load applied = 2Kg = 19.60 N
D=Diameter of disc = 50 mm
N= Fringe order observed at the center of the disc = 2.66

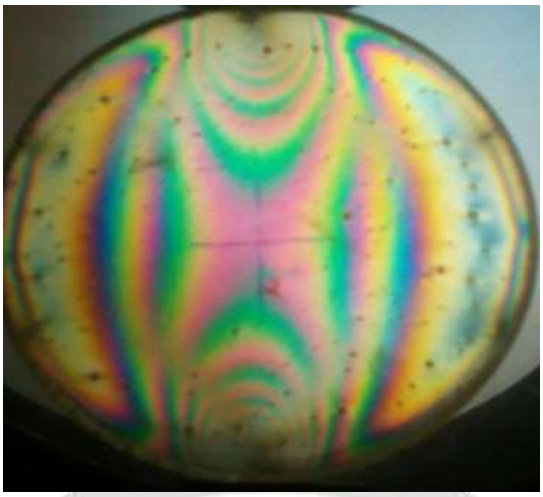

Fig.7:- Stresses Developed in Calibration Disc

Substituting these values in above equation,

$$F\sigma = \frac{8 \times 2 \times 9.81}{\pi \times 50 \times 2.66}$$

$$F\sigma = 0.37 \text{ N/mm}$$

C] Evaluation of Stress at Root of Tooth

According to stress optic law,

$$\sigma_1 - \sigma_2 = \frac{N \times f_\sigma}{t}$$

Where,

σ_1=Major principal stress.

σ_2= Minor principal stress.

N=Fringe order or fractional fringe order.

F_σ=Material fringe order.

t =Thickness of slice.

We know that when a boundary of the model is not loaded directly, it is called free boundary. The normal and shear stresses on a plane tangential to a free boundary are therefore zero. The principal stress axes are normal and tangential to the boundary. One of the principal stresses, say σ_2, is zero. Hence the isochromatic near a free boundary give the values of non-vanishing principal stress σ_1.

$$\sigma_1 = \frac{N \times f_\sigma}{t}$$

Following is the photograph of slice for which analysis of stresses is done. The aim of the project is to evaluate the stresses at the tooth root. Thus tooth root is the point of interest. From the photograph, it is clear that the stresses are concentrated at the tooth root. This is isochromatic fringe pattern in which the green colored fringe can be seen near point of interest i.e. tooth root. The green color is near to the tooth root. If there would have been any color passing exactly from the tooth root, then the respective fringe order would have been taken directly for further calculations. Thus we have to compensate for this. We have to pass that green band from the tooth root. This is done by rotation of analyzer through required degrees. When green band will pass completely through the tooth root, we have to measure the rotation of the analyzer in degrees and from this value we can achieve fractional fringe order.

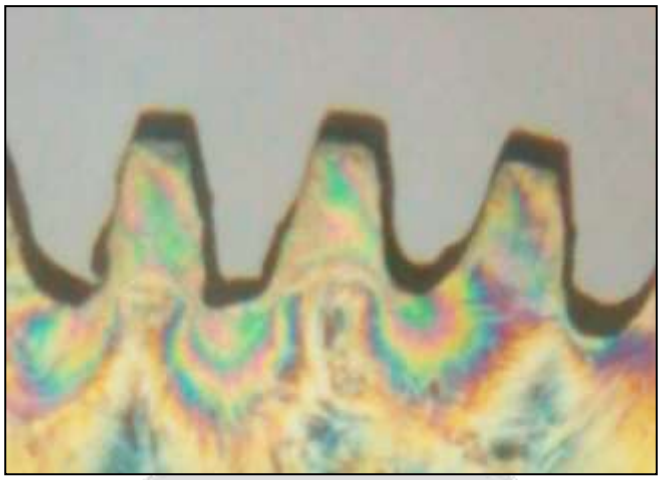

Fig.9:- Fringe Pattern at the Tooth Root

According to Tardy's method of compensation, fractional fringe order N is calculated as,

$N = n \pm (\gamma/180)$ ---------- where n is fringe order.

$N = 2.33 + (70/180)$

$N = 2.718$

Therefore for one slice, the model stresses are calculated as below.

$\sigma_1 = \frac{2.718 \times 0.37}{3} = 0.3353$ N/mm^2

Now, as the load was given throughout the face width, the value of stresses produced in total model is derived as below.

$\sigma_m = \frac{0.3353 \times 25.08}{3}$

$\sigma_m = 2.80$ N/mm^2

D] Scaling Model to Prototype

In the analysis of the photo elastic method of stress analysis, it is tacitly assumed that the prototype structure behaves as a linearly elastic structure within the range of the design load. The photoelastic models reproduce elastic behavior both at the room temperature and stress-freezing temperature used for three-dimensional analysis.

A close examination of the governing equation of the mathematical theory of elasticity shows that for singly connected body, these are entirely independent of the elastic constants, Young's modulus and Poisson's ratio of material in absence of body force or when the body force field is uniform as in case of the gravitational field. In other cases, Poisson's ratio does have a small effect. Even in the case of multiple connected bodies, if the forces around individual openings are such that the resultant force in each case is zero, the stress distribution remains independent of elastic constants. It is thus possible in all practical cases to apply the photoelastic model result to prototype.

Scaling the stresses from model to prototype was carried out as follows.

We have,

$$\sigma_p = \sigma_m \times \left(\frac{T_p}{T_m} \times \frac{h_m}{h_p} \times \frac{L_m}{L_p} \right)$$

Where,

T_p = Torque on a prototype.

T_m = Torque on a model.

σ_p = Stresses produced in prototype.

σ_m = Stresses produced in a model.

h_m = thickness of prototype.

h_m = thickness of model.

L_m =typical lateral dimensions of prototype.

L_m =typical lateral dimensions of model.

As model and prototype have same dimensions.

$h_m = h_p$ and $L_m = L_p$
Therefore,

$$\sigma_p = \sigma_m \times \left(\frac{T_p}{T_m}\right)$$

We have,
Torque on prototype = 33157.27 N-mm
Torque on model = (4×9.81×20) = 784.8 N-mm
Stresses produced in a prototype,

$$\sigma_p = 2.80 \times \left(\frac{33157.27}{784.8}\right)$$

$$\boldsymbol{\sigma_p} = \mathbf{118.29 N/mm^2}$$

The bending stresses of worm wheel obtained by this method are 118.29 N/mm^2. This value is far below the ultimate tensile strength of PB2 material. Hence it can be stated that the design is safe. Also as the analytical stress value is 144.64 N/mm^2, the variation between analytical and experimental analysis is about 18%. This variation is due to the problem in designing and developing the loading frame. During work, it was found that due to high speed reduction (60:1), the load was unable to remain perpendicular at the critical temperature. At critical temperature (80^0 C), there used to be very minor deformation of the wheel material, but due to this, there was noticeable rotation of the worm hence required torque was not properly transferred from worm to the worm wheel.

8.FINITE ELEMENT ANALYSIS-(ANSYS)

Modeling

The tooth of the worm wheel is modeled in Creo 2.0 software from the given 2D drawing. Creo is user friendly software so it is best tool for drawing 3D model.
The image shows the model of the tooth of worm wheel.

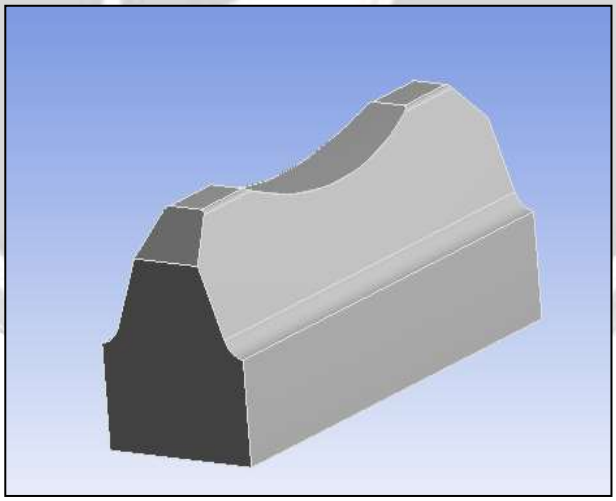

Fig.10:- Creo Model of Tooth of Worm Wheel

Selection of Proper Element for Meshing

In order to carry out a finite element analysis, the model must be divided in to a number of small pieces known as finite element. In simple term, a mathematical net or "mesh" is required to carry out a finite element analysis. If the system is 1D in nature, we may use line element to represent our geometry and to carry out our analysis. If the problem is two dimensions, then a 2D mesh is required. Corresponding, if the problem is complex and a 3D representation of the continuum is required, then we use a 3D mesh. A very fine mesh creates the hardware space problem because the computation becomes voluminous. Out of several kinds of elements, solid elements are used for meshing a 3D component. The shape of solid elements can be a Hexahedron, Wedge, Tetrahedron or a Pyramid as per requirements. Figures below shows the configuration and the number of nodes required for each element.

For meshing a tooth, linear tetrahedron is used. Very fine meshing is used so as to get very accurate results. The size of the element is chosen to be 1 mm.

Number of nodes generated is 1991152 and number of elements generated is 1180999.

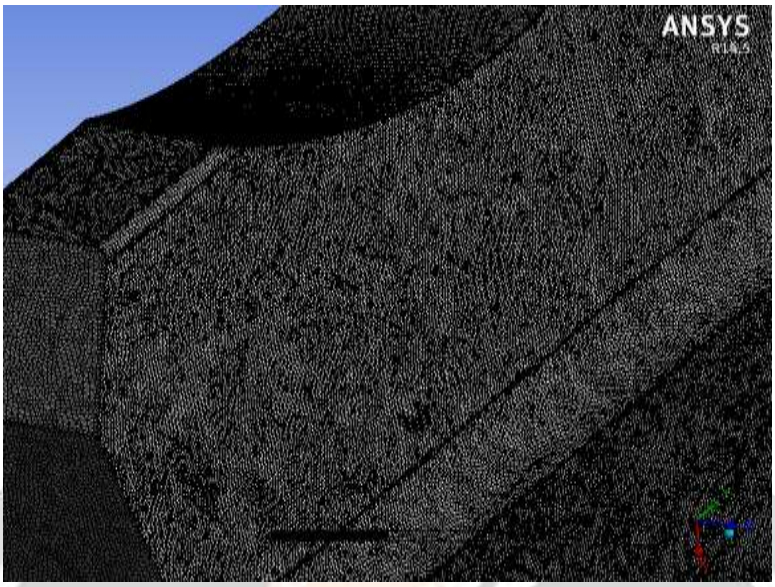

Fig.10:- Meshing of Tooth of Worm Wheel

Specifying Required Inputs

The material of existing worm wheel is Phosphor Bronze 2.Therefore specifying following properties, phosphor bronze PB2 material is selected. Material properties such as Young's modulus (E)**,** Poisson's ratio (ν) are given as input.

Loading and Boundary Condition

The theoretical analysis is carried out using Lewis equation. In the Lewis analysis, the gear tooth is treated as a cantilever beam. Therefore the tooth is fixed at remaining surfaces and load of 16732.57 N is applied at the edge of tooth thus simulating load on cantilever beam. Following figure shows fixed supports and the load applied to the tooth at the tip surface. This indicates that the load is at the end of cantilever beam.

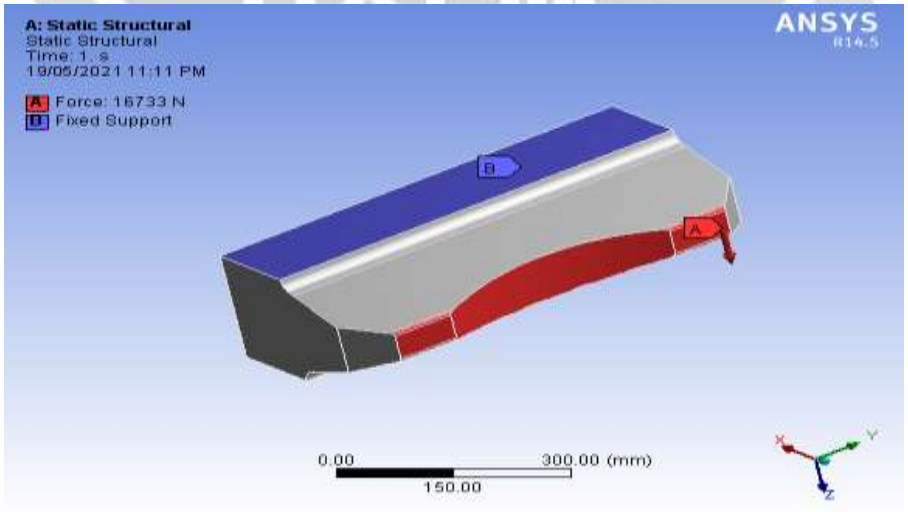

Fig.11:- Loading and Boundary Conditions

Carrying out the Post Process

After applying inputs, loading and boundary conditions, the project should be solved to find out various parameters like total deformation, equivalent stresses, normal stresses, maximum and minimum principal stresses etc.

In this dissertation, as we have to find out the stresses considering Lewis equation, normal stresses along only one direction are taken into consideration. Therefore the model is solved for normal stresses and total deformation. Also the model is solved for equivalent stresses (von-mises stresses).

Plotting the Results

The analysis of worm wheel is carried out by applying above stated loading and boundary condition. The total deformation, normal stresses and equivalent stresses and are shown in figures 22,23,24 respectively.

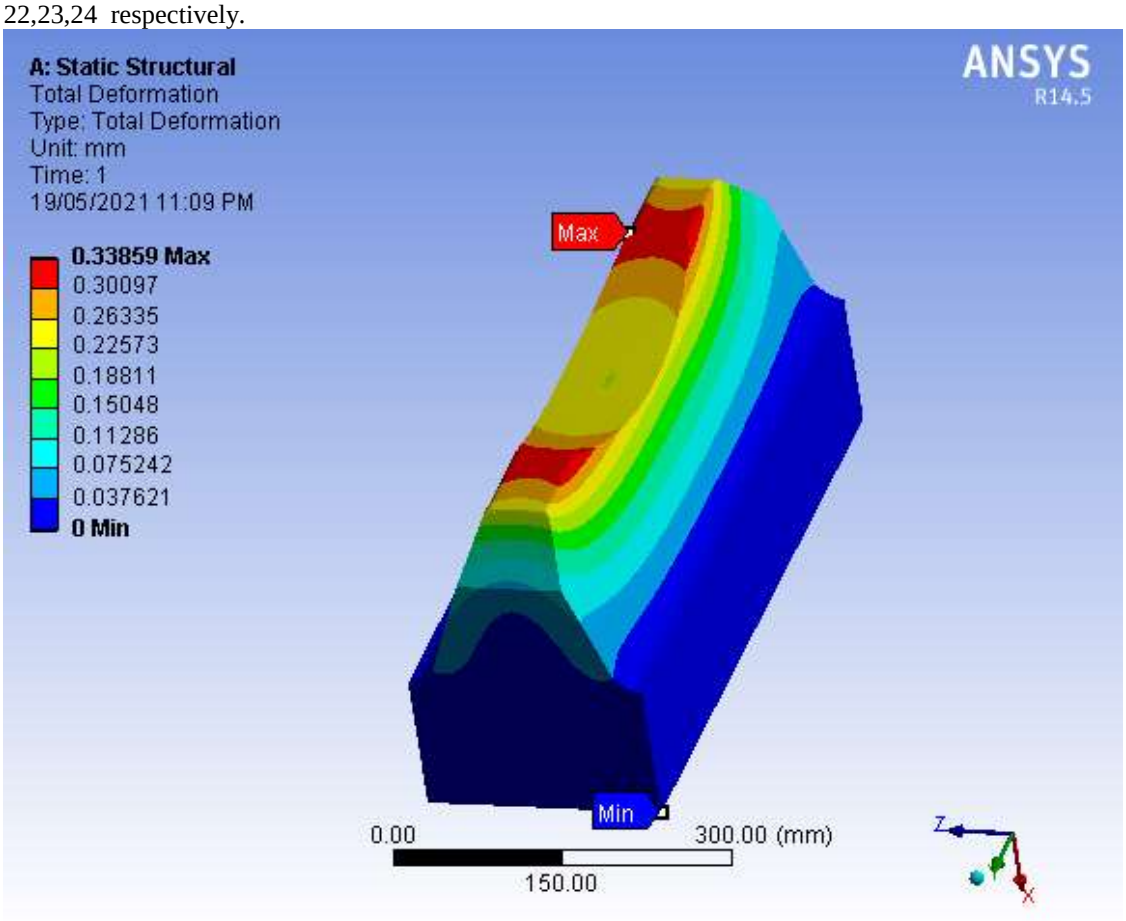

Fig.12:- Total Deformation for Tooth of Worm Wheel

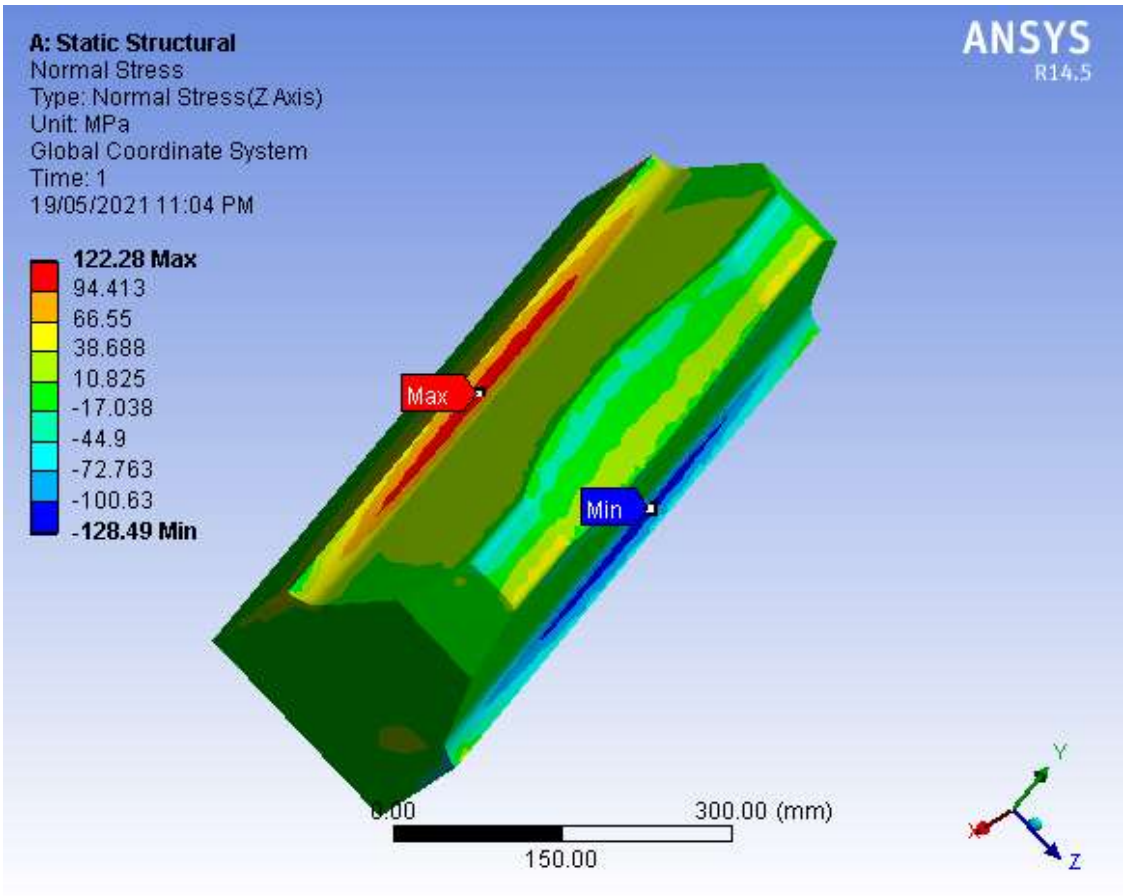

Fig.13:- Normal Stresses for Tooth of Worm Wheel

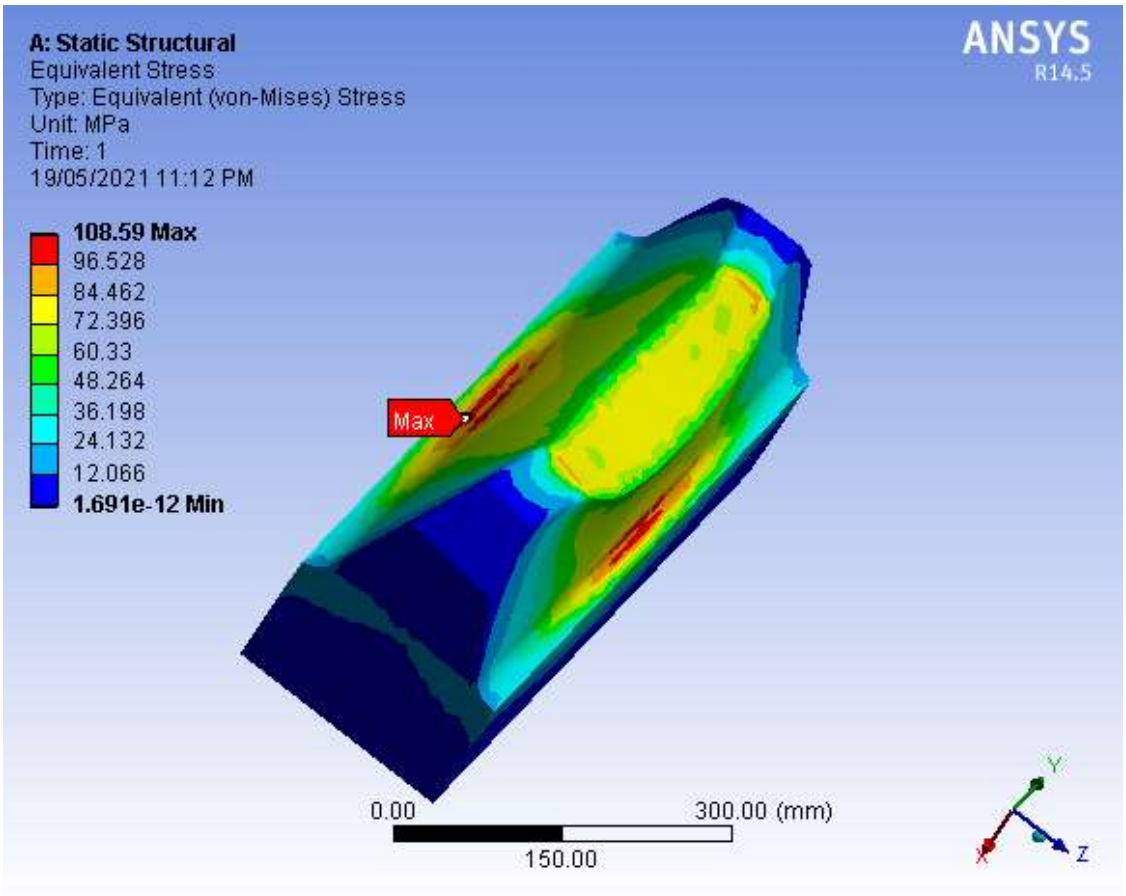

Fig.14:- Von-Mises stresses for Tooth of Worm Wheel

The bending stress value obtained is 122.28 N/mm^2. This value is far below the ultimate tensile strength of the PB2 material. Hence the design is safe. Also from the obtained results, it can be stated that the ANSYS suits to be best method to validate the experimentally obtained results. The variation of theoretical and FE analysis is about 15 %. The variation is due to reason that the FEM is approximate method of analysis.

9.RESULTS AND DISCUSSION

Results of Analysis

The worm wheel is analyzed using theoretical, experimental and finite element method. The following table shows the values of bending stress for each of the analysis.

Bending Stresses by Theoretical Analysis N/mm^2	Bending Stresses by Experimental Analysis N/mm^2	Bending Stresses by FE Analysis N/mm^2
144.64	118.29	122.28

Table2:- Values of Bending Stresses

From the above table it is clear that the design of worm wheel is safe as the ultimate tensile strength of wheel material PB2 is 320 N/mm^2. All the values obtained from each analysis are far below the ultimate tensile strength of wheel material having factor of safety more than 2. Therefore it is clear that the failure of wheel is not due to design parameters but due to some other reasons. Also the hardness of the phosphor bronze PB2 is 110 BH, which is acceptable value, thus it states that the gear material used is suitable for respective application The comparison of experimental analysis and finite element analysis indicates that the variation of results is about 4 % only.

10.Solution

For production of both worm and worm wheel, special production processes are required which are carried out on the special milling machines with special tools. The production of gears on specific machine is costly but the accurate geometry is achieved on gear milling machines only.

Thus as a primary solution, it was decided that the worm should be produced on the milling machine. After production of worm on the lathe machine it found that there is variation in the surface finish as well as geometry of the worm. Hence company accepted the solution on a primary basis. Now the Advance Engineers are producing the worm on gear milling machine and they found the best results with the performance of gearbox.

10.CONCLUSION AND FUTURE SCOPE

Conclusion

By determining the stress analysis by three methods i. e. theoretical, experimental and FE analysis, the following conclusions are made.

1. Though the worm wheel fails during working, the design of worm wheel is safe. Hence the reason for failure may be production method of the mating worm.
2. Among the three methods used for stress determination, the result obtained from FEA are closure to theoretical than experimental results.
3. Designing and developing a loading frame is very important factor in 3D photo elasticity so as to simulate actual loading conditions.
4. FEM and experimental method gives the actual visualization of stress pattern of the component under study.
5. Before going directly for failure analysis of any component, every possible reason should be checked out on primary basis.

Future Scope

1. The present analysis is carried out only for worm wheel. In future analysis may be carried out for the worm.
2. Also thermal analysis can be carried out as heat generation is more during operation.
3. The specific heat treatment can be done to improve the tooth strength.

11.References

[1] Prashant Patil, Narayan Dharashivkar, Krishnakumar Joshi, Mahesh Jadhav. “3D Photoelastic and Finite Element Analysis of Helical Gear”, Machine Design, Vol.3 (2011) No.2, ISSN 1821-1259 pp. 115-120.

[2] Bhosale Kailash C., A.D.Dongare, “Photoelastic Analysis of Bending Strength of Helical Gear”, Innovative Systems Design and Engineering, ISSN 2222-1727 (Paper) ISSN 2222-2871 (Online) Vol. 2, No 3.

[3] W. T. Moody and H. B. Phillips, “Photoelastic and Experimental Analog Procedures”, Engineering Monograph No. 23, United States Department of the Interior Bureau of Reclamation.

[4] Rexnord Industries, LLC, Gear Group, “Failure Analysis Gears-Shafts-Bearings-Seals”, August 1978, pp 1-20.

[5] Dr.V.B.Sondur, Mr.N.S.Dharashivkar, “Theoretical and Finite Element Analysis of Load Carrying Capacity of Asymmetric Involute Spur Gears”, International journal of research in aeronautical and mechanical engineering vol.1, July 2013, pp 67-73.

[6] Pravin M. Kinge, Prof. B.R. Kharde, Prof. B.R. Borkar, “Stress Analysis of Gearbox”, IRACST – Engineering Science and Technology: An International Journal (ESTIJ), ISSN: 2250-3498, Vol.2, No. 3, June 2012, pp 367-371.

[7] Gavril Ion, “Tooth's Tensions Analysis of Face Worm Gears with Cylindrical Pinion Development of FEA”, Scientific Bulletin of the Petru Maior University of Tirgu Mures Vol. 6 (XXIII), 2009 ISSN 1841-9267.

[8] William L. Janninck, “The Contact Surface Topology of Worm Gear Teeth”, available on www.geartechnology.com.

[9] Gitin M. Maitra, “Handbook of Gear Design”, Tata McGraw Hill Publication Company limited. pp 4.1-4.43.

[10] V.B. Bhandari, “Design of Machine Elements”, Tata McGraw Hill Publication Company limited, third edition, pp 730-748.

[11] Faculty of Mechanical Engineering, PSG College of Technology, Coimbatore, "Design Data, Data Book of Engineers", Kalaikathir Achchagam publications. 8.43-8.54.